one CH_3 of the $C(CH_3)_3$ group can lie on a consignate path; the others must lie on dissignate paths and make anti-octant contributions. The axial *tert*-butyl isomer **1** in marked contrast behaves very differently from the 4(a)-methyladamantan-2-one counterpart in giving surprisingly *strong*, negative n–π^* CEs at room temperature, $\Delta\epsilon_{296}^{max}$ −0.29 (MI), $\Delta\epsilon_{296}^{max}$ −0.54 (EPA), vs. weak, variable CEs, $\Delta\epsilon_{301}^{max}$ +0.023 (MI), $\Delta\epsilon_{306}^{max}$ −0.046, (EPA) of the latter. As with the equatorial *tert*-butyl ketone, the CEs are essentially temperature invariant down to −175 °C, again in marked contrast to the axial CH_3 analogue, for which the CE magnitude increases 10-fold at −175 °C, with sign inversion in MI solvent.[14] Thus, the β-axial *tert*-butyl group behaves as a *strong front octant perturber* that is insensitive to solvent and temperature effects.

Molecular mechanics (MM2)[16] calculations predict a higher energy (1.5 kcal/mol higher) for the sterically more crowded equatorial isomer. Using the adamantanone model, one might therefore assume that although still large the conformational energy difference between chair conformers of 3-*tert*-butylcyclohexanone is less (~3.9. kcal/mol) than the computed *A* value (~5.4 kcal/mol) for *tert*-butylcyclohexane.[17]

Acknowledgment. We thank the National Science Foundation (CHE 8218216) for generous support of this work and Dr. S. L. Rodgers for carrying out the MM2 calculations of **1** and **2**.

(15) Kirk, D. N.; Klyne, W. *J. Chem. Soc., Perkin Trans 1* **1974**, 1076–1103.
(16) Allinger, N. L.; Yuh, Y. Y. *QCPE* 423 (Adapted for CDC by S. Profeta), Quantum Chemistry Program Exchange, Indiana University, Bloomington, IN.
(17) Wertz, D. H.; Allinger, N. L. *Tetrahedron* **1974**, *30*, 1579–1586.

High-Speed Spatially Resolved High-Resolution NMR Spectroscopy

Shigeru Matsui,* Kensuke Sekihara, and Hideki Kohno

Central Research Laboratory, Hitachi Ltd. Kokubunji, Tokyo 185, Japan

Received December 10, 1984

Several methods have been proposed[1–4] for high-resolution NMR spectroscopic study of spatially inhomogeneous objects, such as biological systems. Among these, the most general and practically useful method appears to be the method employing the multidimensional Fourier transform (FT) NMR techniques,[3] where two- or three-dimensional spatial information is phase-encoded into free induction decays by pulsed applications of field gradients.[5] This type of method, however, is extremely time consuming, because a large number of measurements, which ensure the required resolution in the multidimensions, must be made to obtain full information.

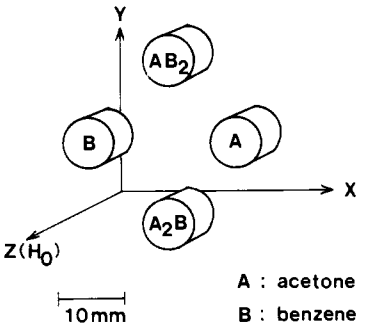

Figure 1. Two-dimensional test sample consisting of acetone (A) and benzene (B). A relaxation reagent, iron(III) acetylacetonate, was added so as to shorten the spin–lattice relaxation times down to about 100 ms for experimental convenience. Each cylinder has a diameter of 8 mm and a length of 10 mm. A, B, AB_2, and A_2B denote the constitutions of the solutions.

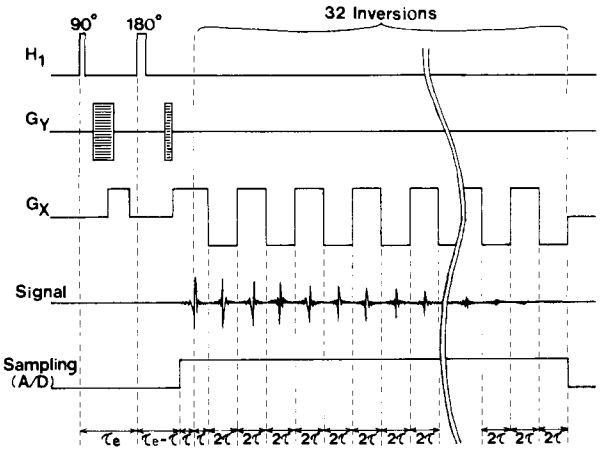

Figure 2. Pulse sequence for high-speed spatially resolved high-resolution NMR spectroscopy. A spatially two-dimensional version is shown. The spin–echo method is employed for compensating the finite-switching-time effects of the field gradient and for observing the initial halves of the first echoes in the echo train signals. The rf pulse interval τ_e = 10 ms. 32 echoes were induced by successive inversions of the field gradient, G_X = 6.8 mT/m, with τ = 1.248 ms and the switching time $\simeq$ 50 μs. Echo trains phase encoded by stepwise applications of the field gradient, G_Y = 6.8 mT/m (the effective phase-encoding time = 1.248 ms), were sampled with an analog-to-digital conversion rate of 78 μs using 1024 points, starting at time $2\tau_e - \tau$.

We wish to describe here our experimental results on a high-speed method of spatially resolved high-resolution NMR spectroscopy, which is closely related to the chemical-shift-resolved NMR imaging methods theoretically described by Mansfield[6a,b] recently. In our method, however, spin–echo trains induced by periodical inversions of a field gradient[6] are further phase modulated (phase encode)[5] by pulsed applications of other field gradients.[7] Such phase-modulated spin–echo trains can be converted to three- or four-dimensional data including both spectroscopic and spatial information by means of suitable data manipulation involving echo rearrangement[6,8] and multidimensional Fourier transformation. Since two-dimensional information (spectroscopic and spatial) can be extracted from each one-dimensional spin–echo train, the dimension of the measurement can

(1) (a) Lauterbur, P. C.; Kramer, D. M.; House, W. V., Jr.; Chen, C. N. *J. Am. Chem. Soc.* **1975**, *97*, 6866. (b) Bendel, P.; Lai, C. M.; Lauterbur, P. C. *J. Magn. Reson.* **1980**, *38*, 343.
(2) (a) Ackerman, J. J. H.; Grove, T. H.; Wong, G. G.; Gadian, D. G.; Radda, G. K. *Nature (London)* **1980**, *283*, 167. (b) Gordon, R. E.; Hanley, P. E.; Shaw, D.; Gadian, D. G.; Radda, G. K.; Styles, P.; Bore, P. J.; Chan, L. *Nature (London)* **1980**, *287*, 736.
(3) (a) Brown, T. R.; Kincaid, B. M.; Ugurbil, K. *Proc. Natl. Acad. Sci. U.S.A.* **1982**, *79*, 3523. (b) Maudsley, A. A.; Hilal, S. K.; Perman, W. H; Simon, H. E. *J. Magn. Reson.* **1983**, *51*, 147. (c) Pykett, I. L.; Rosen, B. R. *Radiology (Easton, Pa.)* **1983**, *149*, 197. (d) Hall, L. D.; Sukumar, S. *J. Magn. Reson.* **1984**, *56*, 314.
(4) (a) Lauterbur, P. C.; Levin, D. N.; Marr, R. B. *Radiology (Easton, Pa.)* **1983**, *149P*, 255. (b) Lauterbur, P. C.; Levin, D. N.; Marr, R. B. *J. Magn. Reson.* **1984**, *59*, 536.
(5) (a) Kumar, A.; Welti, D.; Ernst, R. R. *J. Magn. Reson.* **1975**, *18*, 69. (b) Edelstein, W.; Hutchison, J.; Johnson, G.; Redpath, T. *Phys. Med. Biol.* **1980**, *25*, 751.

(6) (a) Mansfield, P. *J. Phys. D* **1983**, *16*, L235. (b) Mansfield, P. *Magn. Reson. Med.* **1984**, *1*, 370. (c) Mansfield, P. *J. Phys. C* **1977**, *10*, L55. Rearrangement in the frequency domain equivalent to the echo rearrangement is described.
(7) Our method coincides with Mansfield's methods[6a,b] in the case of one-dimensional objects. For two- or three- dimensional objects, however, his methods necessitate two or three inverting field gradients or rotation of a inverting field gradient. Particularly in view of practical applicability our method possesses important advantages over his methods.
(8) This type of rearrangement has also been discussed in other applications of NMR: (a) Waugh, J. S.; Maricq, M. M.; Cantor, R. *J. Magn. Reson.* **1978**, *29*, 183. (b) Terao, T.; Matsui, S. *Phys. Rev. B* **1980**, *21*, 3781.

0002-7863/85/1507-2817$01.50/0

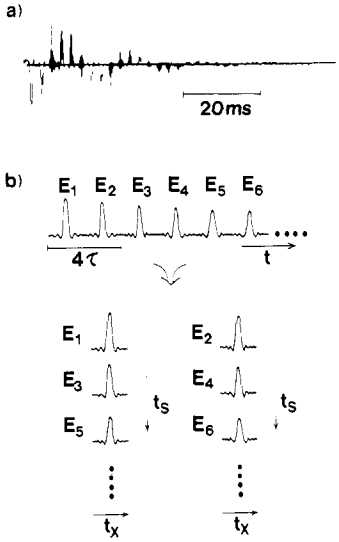

Figure 3. (a) Representative echo-train signal observed by applying the pulse sequence shown in Figure 2. Note that (i) each echo shape is governed by the field gradient G_X, yielding the spatial information, and (ii) the echo envelope corresponds to the normal free induction decay giving the high-resolution spectrum. (b) Rearrangement of echo trains. Odd- and even-numbered echoes are separately rearranged to give two sets of two-dimensional arrays, in which the time axis t_S corresponds to the spectral axis and the time axis t_X to the spatial axis X.

be reduced by one in comparison with the usual multidimensional FT method.[3]

Experiments were performed at 0.5 T, operating our NMR imager[9] for protons. Figure 1 shows our two-dimensional test sample consisting of acetone (A) and benzene (B); the proton chemical-shift difference is 5.1 ppm. The pulse sequence used for the measurement is schematically shown in Figure 2. If a periodically inverting magnetic field gradient G_X is imposed on a sample during observation of a free induction decay, the resultant signal takes the form of a spin–echo train as shown in Figure 3a. Such an echo-train signal is modulated by both internal magnetic interactions within the sample, which give high-resolution spectra, and an external interaction generated by the time-dependent field gradient, which provides one-dimensional spatial information X. Consequently, the two distinct types of information can be extracted from the single echo train.[6,8] Furthermore, remaining spatial information Y can be phase encoded[5] into the echo-train signal by pulsed applications of a field gradient G_Y. In each phase-encoded (or phase-modulated) echo train, odd- and even-numbered echoes are separately rearranged to give two sets of two-dimensional arrays as shown in Figure 3b;[8a] along the new time axis t_S, one can observe free induction decays which give high-resolution spectra, because the effects of the external interaction on the signals are quenched along the new time axis.[10] The echo shapes are governed by the external interaction (G_X), which is represented on the t_X axis (Figure 3b). Since the spatial information Y is already phase-encoded along the third axis t_Y perpendicular to both array axes t_S and t_X, three-dimensional Fourier transformation of either set of the three-dimensional rearranged data (t_S, t_X, t_Y) can yield chemically resolved proton images and spatially resolved proton high-resolution spectra as shown in Figure 4. It should be noted that the two sets of three-dimensional FT data can mutually be coadded after correcting the sign difference in X.[6a,b] For three-dimensional objects, another phase encoding and Fourier transformation are necessary along the Z direction.

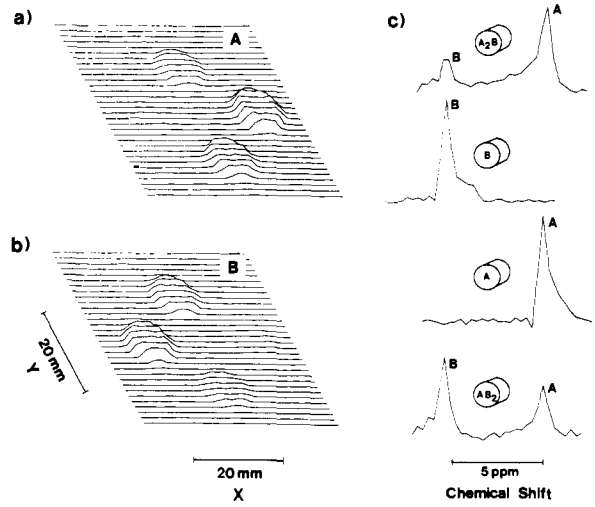

Figure 4. Proton images of acetone (a) and benzene (b), and proton high-resolution spectra at four different locations (c). Two echo trains were added in each step of 32 phase encodings with a repetition time 500 ms, the total measurement time being only 32 s. Both the X and Y axes are represented by 32 points and the spectra by 32 points, interpolated from 16 points using the zero-filling technique; the number of spectral data points is limited by the memory size of our signal averager (1024 points). The images were obtained from the spectral intensities of absolute values of the Fourier transforms while the local spectra are of phase-corrected absorption mode. The use of absolute values can solve a dephasing problem caused by homonuclear J couplings. Each local spectrum shifts depending upon the field strength at the corresponding location with the spectral separation preserved. The spectral resolution of each local spectrum is limited by the corresponding local field inhomogeneity,[11] as in the multidimensional FT method.[3b,c]

Acknowledgment. We thank Hidemi Shiono for his skillful help in assembling a signal-acquisition program.

(9) (a) Matsui, S.; Yamamoto, E.; Kuroda, M.; Shiono, H.; Kohno, H.; Ohtomo, H.; Kato, H.; Kogure, K., Proceedings of the 22nd NMR symposium in Japan, Kyoto, Japan, Nov 1983. (b) Kato, H.; Kogure, K.; Ohtomo, H.; Tobita, M.; Matsui, S.; Yamamoto, E.; Kohno, H. *J. Cereb. Blood Flow Metab.*, in press.

(10) To realize this quenching experimentally, precise timing adjustment was made for the inversions of the field gradient G_X so that the field-gradient effect on spin phases is always cancelled at times $2\tau_e + 2N\tau$ ($N = 0, 1, 2, 3, \ldots, 31$) (see Figure 2).

(11) It may be worth noting that if the object is in fact spatially homogeneous, all the local spectra can be coadded after correcting the spectral shifts; therefore, spectral broadening due to overall field inhomogeneity is avoidable even if the sample is very large.

Kinetic Isotope Effect in Gas-Phase Base-Induced Elimination Reactions

Veronica M. Bierbaum,* Jonathan Filley, and Charles H. DePuy

Department of Chemistry, University of Colorado Boulder, Colorado 80309

Martin F. Jarrold and Michael T. Bowers*

Department of Chemistry, University of California Santa Barbara, California 93106

Received December 5, 1984

Most exothermic gas-phase ion–molecule reactions are rapid, occurring at essentially every collision. This arises because long-range electrostatic forces exist between the ion and neutral; these species, therefore, attract one another and interact with sufficient energy to surmount many traditional barriers to reaction. Nevertheless, there is increasing evidence that these processes can be highly specific. We wish to report the observation of a dramatic example of reaction selectivity: a hydrogen/deuterium isotope effect of 5.5, which is close to the theoretical maximum, in the elimination reaction of amide ion with diethyl ether. Modeling both the absolute rate and isotope effect using statistical rate theory provides insight to the barrier height and reaction mechanism for this process.

0002-7863/85/1507-2818$01.50/0